CLUSTERIZATION IN TWO-DIMENSIONAL SYSTEM OF HARD SPHERES

Agnieszka Chrzanowska, Grzegorz Traczuk, Piotr Fornal

Institute of Physics, Cracow University of Technology
Podchorążych 1, 30-084 Kraków, Poland

(Received April 11, 2007; revised version received July 18, 2007)

A clusterization process in two-dimensional system of granular hard disks is investigated by two novel numerical methods: the nearest neighbourhood density and the anti-percolation function. The tendency of the band like structures in the clustered state is recognized to be driven by two factors: the stretching forces at the junction of two clusters (or two parts of one cluster) with different kinetic energies and the density fluctuations, which act as a seed for the empty ponds (voids free of particles). Moreover, the examples (and animations) of the collision of two clusters and the breakup of the granular band are presented.

PACS numbers: 45.70.–n, 45.70.Qj, 45.70.Vn

1. Introduction

Granular media are an interesting subject, which in the last years attracted a lot of attention [1–4]. The most popular example among different cases of granular matter is the system of two-dimensional spheres (or hard disks) [5, 6]. The reason of such a choice is the simplicity of the collision principles and two-dimensional presentation. In general, the word "granular" applies to the situations, when the colliding particles lose their kinetic energy during collisions because of the friction. This property solely leads to many new interesting phenomena as compared to classical gases. Most striking here is the growth of clusters [5–11], which are the areas, where the particles gather if they have not enough kinetic energy to escape from their collisional partners. At the same time one observes occurrence of large voids free of particles. Other phenomena observed are the shear bands, which are present in early stages of cooling, when the system is still homogeneous and clusters migrations. During simulations, especially for strong dissipation, one can encounter also the inelastic collapse, *i.e.* the situation, when the collision frequency becomes divergent. This, however, is an artefact of

the simulations under the constraint of the binary collisions and is symptomatic for the fact that multiparticle collisions are inherent to the granular condensed matter.

The most crucial parameter in granular gases, besides the density, is the so-called restitution parameter r, which gives, depending on the model, either the fraction of the contact velocity or the fraction of the momentum exchange that is preserved during the collision. According to the value of the restitution parameter for the contact velocity in the system of 2D hard disks McNamara *et al.* [5] have recognized four different regimes of the dynamical state: kinetic, shearing, clustered and collapsed. In the kinetic regime, where $0.98 \leq r \leq 1.0$ (in this model r is connected to the contact velocity), the configurations made of the disks are structureless and resemble the case of a classical nondissipative gas. For $0.83 \leq r \leq 0.97$ the system evolves into the shearing state. This state has been first described by Goldhirsch and Zanetti [7]. It is characterized by the fact that most of the energy and momentum resides in the hydrodynamic shearing mode, whereas the density does not exhibit inhomogeneities. On can imagine here two counterflowing streams, whose global motion contains a large fraction of the total kinetic energy. It has turned out that the transition from the kinetic to the shearing state can be well described by the kinetic theories [7,8,12,13]. According to these theories predictions, the presence of the shearing mode is determined by the competition between the dissipation of thermal energy by the inelastic collisions and the rate at which the viscosity transfers the macroscopic kinetic energy into the thermal energy. This may happen, for instance, if we introduce a short wavelength shear wave into the system that finds itself in the kinetic regime. In this case the viscous forces will quickly transfer the macroscopic energy of the wave into the thermal energy and then, as a consequence, the system enters the purely kinetic regime again.

In the kinetic regime the energy of the system calculated after the same number of collisions strongly depends on the restitution parameter; in the shearing regime it is nearly independent on r. Smaller values of r, $0.59 \leq r \leq 0.82$, lead to the clustered state with the pronounced cluster formation and no shearing mode features. In this state the particles are gathered into clusters, which collide, breakup and reorganize [8]. Many attempts have been undertaken to describe its properties like, for instance, the size or number of the clusters [6]. For the values of r smaller than 0.58 the simulated system can enter once again the shearing state (and seems to remain in this state) or evolve directly into the collapsed state. The collapsed state, also known as the inelastic collapse, is characterized by the infinitely large collision rate dN/dt (the number of collisions per unit of time). In practice this means that the computer simulation no longer makes progress. For $r < 0.62$ the probability of inelastic collapse is large, whereas for $r > 0.62$ the simulations

stopped by the inelastic collapse are, if ever, occasional. It is also worth noting that the collapsed state, in which more than two particles are at contact, is dominated by the linear arrangements of the particles involved.

The above categories have been proposed on the basis of the behavior of the $N = 1024$ particles system at the solid fraction $\nu = 0.25$ ($\nu = N\pi\sigma^2/(4L^2)$, with L being the size of the simulation domain) within the simulations runs of the length corresponding to 800 collisions per particle. Note, however, that the systems, which are initially in the kinetic or shear regimes, after longer simulations can also enter the clustered or the collapsed states. Everything depends on the amount of energy that is still preserved in the system.

As concerns the driving force of the origin of the clusterization process, it can be found two different explanations in the literature. In [7] Goldhirsch *et al.* indicate the nonlinear shear mode hydrodynamic effects, which dominate the system dynamics, as the main factor responsible for the density inhomogeneity. Another explanation can be found, for instance, in [14, 15], where the initial density fluctuation is just a linear effect associated with the fluctuation of the mode governing the linear evolution of the longitudinal component of the flow field. On the basis of the Monte Carlo solutions of the inelastic Boltzmann equation in [16] Javier Brey *et al.* have given strong argument for the first explanation.

However satisfied one can be with these theoretical analysis of the origin of clusterization, the description of the clusters themselves poses big difficulty, especially the question how to differentiate among different stages of the clusterizations process. In [6] Luding *et al.* have proposed an algorithm, on the basis of which it is possible to describe the evolution of the clusters sizes. In this approach the size of the cluster is calculated according to the rule that two particles belong to the same cluster, if the distance between them is smaller than $s = 0.1$ of the particle diameter. Then the evolution can be investigated using the moments M_k of the cluster size distribution

$$M_k = \frac{1}{n_c} \sum_i i^k n_i \,, \tag{1}$$

where n_c denotes the total number of clusters and n_i the number of clusters of size i. Upon enlarging of the clusters, M_k increases until they reach a saturation value (with large fluctuations).

The current paper provides another two numerical tools by the use of which one can describe different degrees of the system clusterization. The paper is organized as follows. After introduction in Section 1, we present the event driven method for the molecular dynamics simulations together with two models of dissipation, the contact velocity model and the momentum exchange model (Section 2). Next, Section 3 presents the results for the

collision number obtained for the evolutions of 2D hard spheres with different strengths of dissipation. In this paper, however, we do not compare any theoretical results to the simulation data. Instead we propose useful numerical methods for analyzing cluster formation. In particular we apply the concept of the nearest neighborhood density from [17] (Section 4) and introduce the anti-percolation function P (Section 5), which estimates the transparency of the configuration to "the radiation" composed of the hard particles of different sizes. If the statistics is large enough or, equivalently, if the size of the system is large, the above functions are smooth and exhibit regular features, which correspond to different states of clustering. Moreover, we present the illustrations (and appropriate time animations) of two characteristic phenomena from the clustered state, *i.e.* a collision of two clusters (Section 6) and the breakup of the band-cluster (Section 7). The summary and discussion of results are given in the last section.

2. Event driven simulations

The method used in the current work is based on the "event driven algorithm" [5, 18–21], which is suitable for hard particles, as compared to the standard molecular dynamics of soft particles [22, 23]. In our simulations we consider a system of $N = 90000$ two-dimensional circular hard disks in a doubly periodic domain, in which the particles collide with each other under the constraint of a binary collision. The disks have diameter $\sigma = 0.001666$, so the overall reduced density $\rho^* = N\sigma^2/L$ (L — the area of the simulation box is here 1) is equal to 0.25. The simulations are performed according to the event driven molecular dynamics [5, 20, 21]. This method is based on the fact that knowing the positions and velocities of all the particles it is possible to foresee the time $\tau_{\rm col}$ needed to the nearest collision. If there are no external forces, the hard particles between collisions move at a constant velocity, so calculating the particles new positions after the time $\tau_{\rm col}$ is a simple task. Then, because of the binary collision assumption, two particles from the system are *exactly* at contact. At this stage of simulation one applies the formulas imitating collision between these particles. Since the system considered consists of the objects interacting via the hard core potentials, the collision formulas simply predict the velocities and momenta after the collision by the use of the conservation of momentum and the principle for the energy transfer. In the elastic case the energy, of course, must be preserved. For hard spheres this means that the relative velocity of the particles $\boldsymbol{V}_{12}^{\parallel}$, which lies within the plane that is tangent to the bodies at the point of contact, remains unchanged, whereas the velocity normal to this plane, $\boldsymbol{V}_{12}^{\perp}$, is reversed. The concept of "the granular system" assumes the loss of energy during the collisions. This, in practice, can be realized

in two ways: (a) by imposing that the relative velocity perpendicular to the mentioned tangent plane after the collision is not only reversed but also diminished (contact velocity model) by the fraction according to the restitution parameter r (b) by reduction of the momentum exchange (momentum exchange model) according the fraction number r_M.

In our simulations the initial configurations for the granular case are obtained from the molecular dynamics of the elastic disks system performed in the standard way. At first, one prepares a system by placing the particles on a regular array (to avoid mutual overlaps) and by assigning random velocities. Next, the velocities are adjusted to conform to the temperature $kT = 1$ and to the condition that the system as a whole is at rest, *i.e.* that the total momentum is zero. Then, the MD simulation is initiated and runs until one obtains a thermalized state, in which the velocities of the particles are distributed with a Maxwellian velocity distribution. Independent initial configurations for the granular case are generated by stopping the simulations of the elastically interacting disks at different times. The system considered consists of $N = 90000$ of the diameter σ placed in the rectangular simulation box with doubly periodic boundary conditions, which, to some extent, mimics the bulk system of the infinite size. This condition results in the following fact: when a particle leaves the right (or bottom) side of the box, its twin image reenters the left (or top) side. In this manner also the number of particles is kept constant.

2.1. Contact velocity model

The crucial parameter in this model is the restitution parameter r, which gives the fraction of the velocity preserved.

$$\boldsymbol{V}_{12}^{\perp\,\prime} = -r\boldsymbol{V}_{12}^{\perp}\,. \tag{2}$$

The sign $\perp$ denotes here that only the velocities perpendicular to the tangential surface at the point of contact are taken into account. At the same time the relative tangential velocity does not change during a collision (the particles slide over each other). The possible values of r remain within the interval $[0.0; 1.0]$. The particular velocities after the collision can be written as:

$$\boldsymbol{v}_1{}' = \boldsymbol{v}_1 - \tfrac{1}{2}(1+r)\left[\hat{\boldsymbol{k}}\cdot(\boldsymbol{v}_1-\boldsymbol{v}_2)\right]\hat{\boldsymbol{k}} \tag{3}$$

and

$$\boldsymbol{v}_2{}' = \boldsymbol{v}_2 + \tfrac{1}{2}2(1+r)\left[\hat{\boldsymbol{k}}\cdot(\boldsymbol{v}_1-\boldsymbol{v}_2)\right]\hat{\boldsymbol{k}}\,, \tag{4}$$

where $\boldsymbol{k}$ is the unit vector normal to the tangent surface to the bodies at the point of contact. This model has been used, for instance, in [5].

2.2. Momentum exchange model

In the momentum exchange model one utilizes the exchange of momentum that is valid for the elastic case $\Delta \boldsymbol{P}_{\text{elas}}$. Then the effective momentum exchange in the granular case is given as

$$\Delta \boldsymbol{P}_{\text{granul}} = r_M \Delta \boldsymbol{P}_{\text{elas}} \,. \tag{5}$$

The possible values of r remain here within the interval $[0.5; 1.0]$. The upper limit $r_M = 1.0$ corresponds to the elastic case and the lower limit $r_M = 0.5$ describes the event, when the particles are at contact. If $r_M < 0.5$, then the particles are overlapping immediately after the collision. This case is rejected as nonphysical.

The principle of the momentum conservation is

$$\boldsymbol{P}_2{}' = \boldsymbol{P}_2 - \Delta \boldsymbol{P}_{\text{elas}} \,, \tag{6}$$

$$\boldsymbol{P}_1{}' = \boldsymbol{P}_1 + \Delta \boldsymbol{P}_{\text{elas}} \tag{7}$$

and the conservation of the energy (if the particles have the same mass)

$$\boldsymbol{P}_1'{}^2 + \boldsymbol{P}_2'{}^2 = \boldsymbol{P}_1^2 + \boldsymbol{P}_2^2 \,, \tag{8}$$

where

$$\Delta \boldsymbol{P}_{\text{elas}} = \boldsymbol{P}_2 - \boldsymbol{P}_1 \,. \tag{9}$$

Now the exchange model for the granular case assumes that

$$\Delta \boldsymbol{P}^{\perp}_{\text{granul}} = r_M \Delta \boldsymbol{P}^{\perp}_{\text{elas}} \,. \tag{10}$$

As a result the formulas for the postcollisional momenta follow as:

$$\begin{aligned} \boldsymbol{P}_2' &= \boldsymbol{P}_2 - r_M \hat{\boldsymbol{k}} \cdot (\boldsymbol{P}_2 - \boldsymbol{P}_1) \hat{\boldsymbol{k}} \,, \\ \boldsymbol{P}_1' &= \boldsymbol{P}_1 + r_M \hat{\boldsymbol{k}} \cdot (\boldsymbol{P}_2 - \boldsymbol{P}_1) \hat{\boldsymbol{k}} \,. \end{aligned} \tag{11}$$

Finally the postcollisional velocities can be written as

$$\begin{aligned} \boldsymbol{v}_2' &= \boldsymbol{v}_2 - r_M \hat{\boldsymbol{k}} \cdot (\boldsymbol{v}_2 - \boldsymbol{v}_1) \hat{\boldsymbol{k}} \,, \\ \boldsymbol{v}_1' &= \boldsymbol{v}_1 + r_M \hat{\boldsymbol{k}} \cdot (\boldsymbol{v}_2 - \boldsymbol{v}_1) \hat{\boldsymbol{k}} \,. \end{aligned} \tag{12}$$

One observes here that the momentum exchange model and the contact velocity model are equivalent to each other with the relation between their restitution parameters as:

$$r = 2 r_M - 1 \,. \tag{13}$$

3. The collision number

The collision number $N_{\rm col}$ is one of the most important property of the dynamics. For the particles interacting through the elastic forces, when there is no dissipation, this is a linear function in time, the slope of which is given by the collision rate dN/dt. Inclusion of the dissipation results in the departures from linearity and in different collision rates which depend on the current state of the system.

In Fig. 1 we present the behavior of $N_{\rm col}$ obtained from the simulations of $N = 90000$ granular 2D disks performed with different restitution parameters r_M. The thick line corresponds here to the collision number of the elastic disks. One observes then that in the kinetic, shear and also in the clustered states the dynamics is much slower than in the elastic case. Upon diminishing of the restitution parameter the dynamics of the system at the beginning slows down, then the tendency is reversed. The curve for $r_M = 0.8$ is already above the curve for $r_M = 0.9$ and all subsequent curves become gradually steeper. At some stages one observes also the parts, which are almost perpendicular to the t axis. These very steep parts of the collision number $N(t)$ denote here the multiparticle events: either inelastic collapse (the curve for $r_M = 0.51$), when more than two particles are in contact or the collision of two many-particle groups in which the condition of the binary collision still holds (see the inset which corresponds to the part of the curve for $r_M = 0.7$ from the rectangular box). Although the collision between clusters on the $N_{\rm col}$ curve looks very similar to the inelastic collapse, there is an important difference. Looking at the inset on Fig. 1 one sees that when the cluster collision is over, $N_{\rm col}$ becomes again flat.

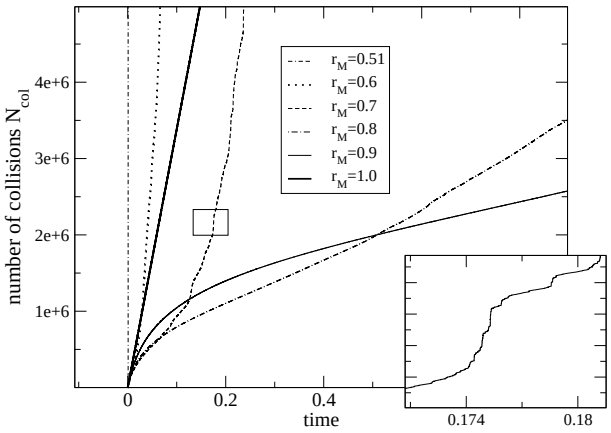

Fig. 1. The number of collisions $N_{\rm col}(t)$ obtained in the simulations with different restitution parameter r_M.

Characteristic is also the behavior of the collision number for strong dissipations, here, for instance, for $r_M = 0.6$ and $r_M = 0.7$. In these cases the dynamics of the system is dominated by large collision rates. At the same time, however, the decay of the system energy is small. These two facts indicate that most of the collision events here take place among the low energy particles, which are placed very close together.

4. The nearest neighborhood density

In Fig. 2 we demonstrate the concept of the nearest neighborhood density $n(\rho^*)$. To each particle from the system we associate a circular box of the radius $R = \alpha\sigma$, where σ is the diameter of the particle. The main particle is assumed to be exactly in the center of the box. The radius R should be taken of no more than few particles dimensions, let us say $\alpha < 10$. Otherwise, if the value of α is too large, the effect of the density inhomogeneities can be averaged out. Next we calculate how many boxes contain a given number of the particles. The statistics presented on the Cartesian coordinate system (upper panel of Fig. 3) turns out to be a regular function, which can be perfectly fitted to the Gauss function. This feature is typical for homogeneous systems, as already presented in [17]. For convenience the number of the particles in the box can be recalculated into the density, then all the Gaussian functions have the maxima almost at the same density, however with different heights and widths (lower panel of Fig. 3).

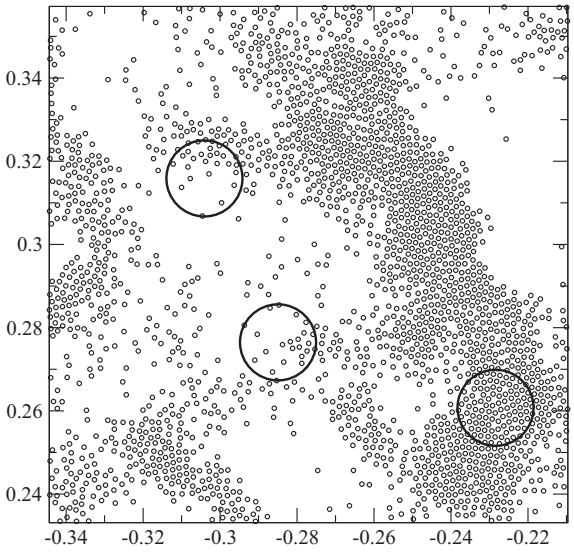

Fig. 2. The concept of the nearest neighborhood density.

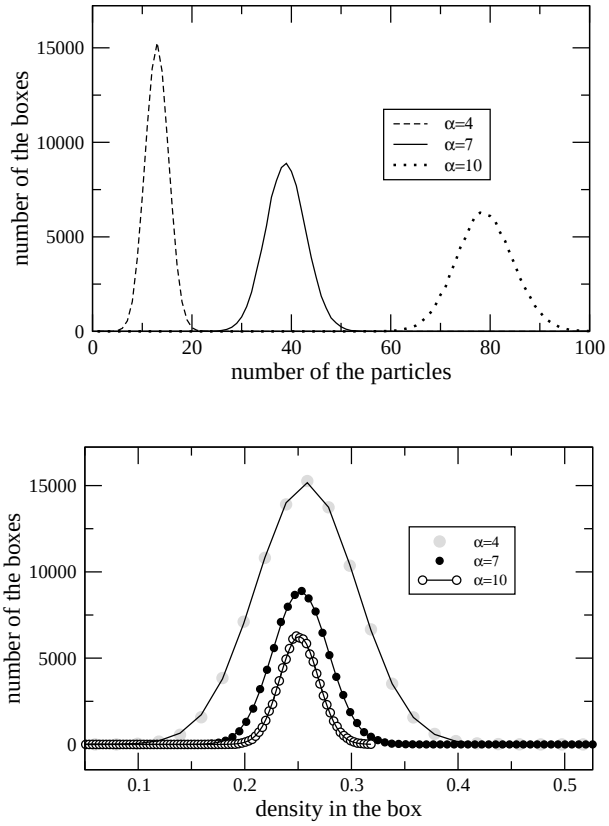

Fig. 3. The nearest neighborhood density distribution of the homogeneous case. The neighborhood box is assumed as circular with the radius R given by the value of α: $R = \alpha\sigma$, where σ is the diameter of the particle. (upper panel) X axis: the number of the particles in the neighborhood box; Y axis: the number of the boxes with the same number of the particles inside. (lower panel) X axis: the density in the box; Y axis: the number of the boxes with the same density. In the lower panel the peaks occur almost at the same density, *i.e.* for: $\rho^* = 0.258$ for $\alpha = 4$, $\rho^* = 0.252$ for $\alpha = 7$, $\rho^* = 0.251$ for $\alpha = 10$.

Figure 4 presents the nearest neighborhood density functions $n(\rho^*)$ obtained in the clustered states of the 2D disks system, which cools down according to the restitution parameter $r_M = 0.9$. In the legends we present the following important values. E is the total percentage measure for the energy per particle. Its value shows how large part of the energy is lost before the clusterization begins. N_{col} is the number of collisions after which the configuration has been considered for the analysis. The corresponding to

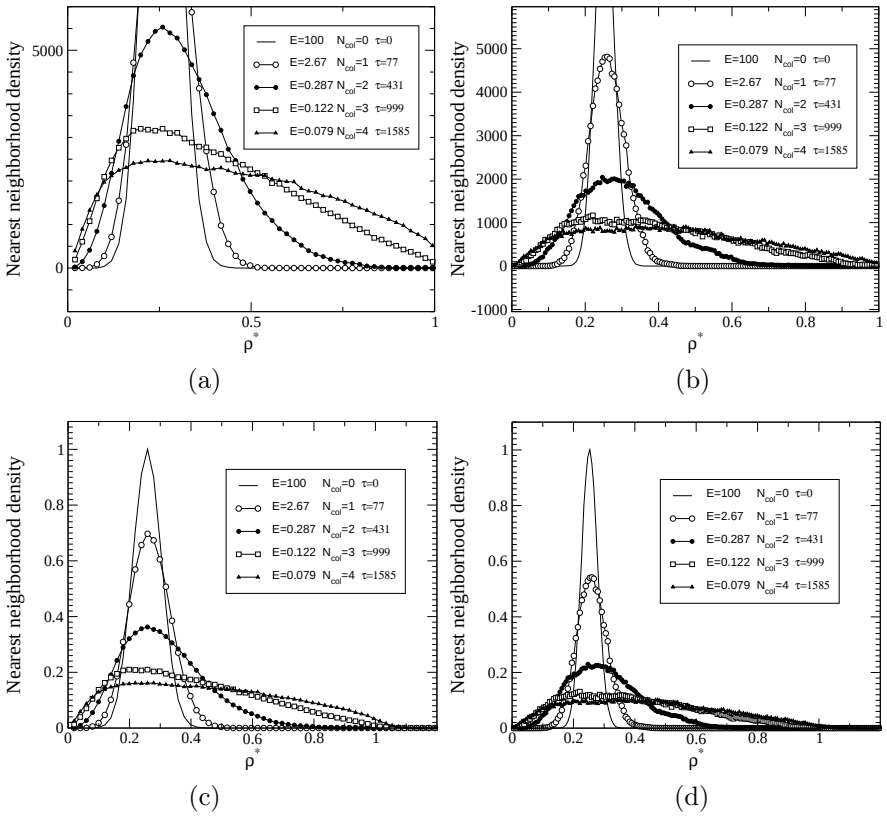

Fig. 4. The nearest neighborhood function obtained at different stages of the evolution of the system with $r_M = 0.9$. In the legends the following values are given: E — the total percentage measure for the energy per particle, N_{col} — the number of collisions after which the configuration has been considered for the analysis and the corresponding to these configurations dimensionless time τ (14). The panels (a) and (c) are for $\alpha = 4$; the panels (b) and (d) are for $\alpha = 7$; In the panels (c) and (d) the axis Y has been rescaled to adjust to the condition that the peak of the Gaussian function for the nondissipated system has the height 1. The function $n(\rho^*)$ is sensitive to the choice of α.

these configurations dimensionless time τ, which had passed till the moment the configuration has been registered, is calculated as the ratio of the actual computational time t_{comp} (which attains its values according to the particle mass, the particle size and the system temperature) to the averaged time needed by a particle to cover the distance equal to its diameter t_{aver}.

$$\tau = \frac{t_{\mathrm{comp}}}{t_{\mathrm{aver}}}\,, \tag{14}$$

where

$$t_{\text{aver}} = \frac{\sigma}{v_{\text{mean}}} = \frac{\sigma}{\sqrt{2E_{\text{kin}}}} = \frac{\sigma}{\sqrt{2kT}}\,. \tag{15}$$

The plots in Fig. 4 are obtained with two diameters of the circular neighborhoods, for $\alpha = 4$ (the panel (a) and (c)) and for $\alpha = 7$ (the panel (b) and (d)), where the neighborhood box diameter $R = \alpha\sigma$.

Upon cooling, when the clusters grow larger, $n(\rho^*)$ becomes asymmetrical with respect to the peak position and this asymmetry strengthens the larger the clusters become. All the obtained profiles exhibit very smooth and regular character, despite the fact that the procedure to construct $n(\rho^*)$, which is of the histogram type, rests on the discrete values of ρ^*.

We have tried also to rescale the figures to see to what extent the presentation is sensitive to the choice of α. The figures in the panels (c) and (d) are recalculated in such a way that the peak of the Gaussian function for nondissipative case is equal to 1. One sees then that the character of the curves is preserved, however the heights of the profiles are different.

The visualization of the configurations corresponding to the profiles from Fig. 4 are given in Fig. 5 and Fig. 6. The pictures of clusters in the panels in Fig. 6 look so similar that one, just looking at them, may not be able to tell the difference of the clusterization degree. The function $n(\rho^*)$, however, is sensitive enough to detect the difference. Look, for instance, at the curve with squares and at the curve with triangles in the panel (a) of Fig. 4.

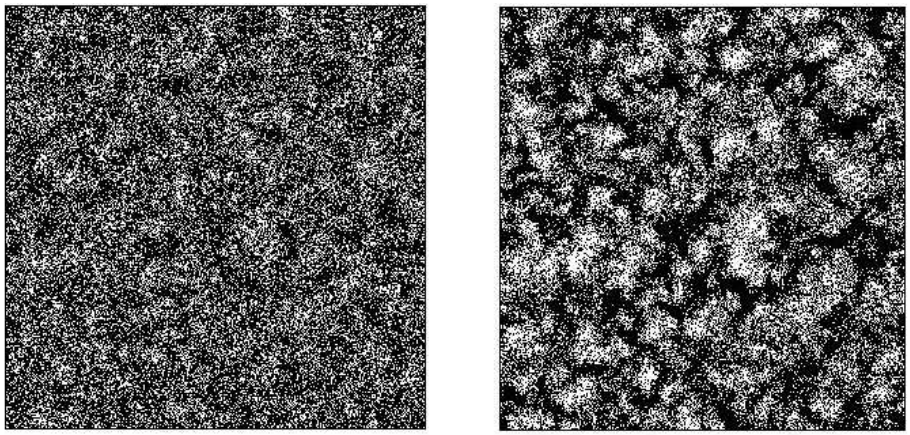

Fig. 5. Configurations obtained after 1 million (the left panel) and 2 millions (the right panel) of collisions. The energy of the system in the left panel is 2.67% of the initial state energy and 0.287% for the configuration in the right panel. The restitution parameter used here is $r_M = 0.9$.

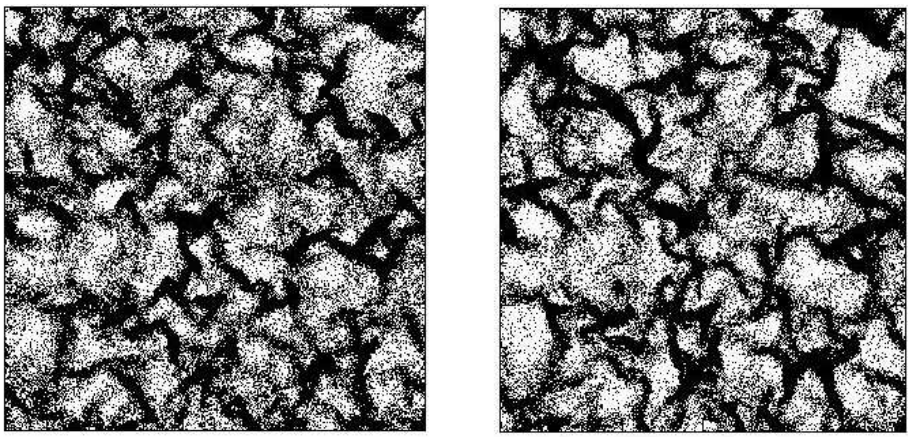

Fig. 6. Configurations obtained after 3 millions (the left panel) and 4 millions (the right panel) of collisions. The energy of the system in the left panel is 0.122% of the initial state energy and 0.0794% for the configuration in the right panel. The restitution parameter used here is $r_M = 0.9$.

5. The anti-percolation function

In this section we would like to introduce the anti-percolation function P as a useful tool to study the clusterization process.

A general idea for this measure is the assessment of the chances that a physical factor can interact with the members of the system. A similar concept can be found in [5], where the authors consider a ray of light that is passing through the system. According to the evaluations from [5], the critical restitution parameters that separate different regimes of the kinetic behavior depend on one physical parameter, which is the so-called *optical length*. Its definition reads:

$$\lambda = \rho^* L = \frac{\sigma}{2}\sqrt{N\pi\,\rho^*}\,. \tag{16}$$

The physical meaning of this property is as follows. Assuming first that the disks are transparent, so the light can pass in an undisturbed way throughout their bodies, one imagines next a ray passing directly across the system, from one boundary to the other. The fraction of the area covered by disks is given by ν, so νL corresponds to the distance over which the ray travels *inside* the particles. This is also the reason that the name "optical path" is in use. For the case in which the simulation box has the side equal to 1, the optical length parameter λ coincides with the reduced density ρ^*.

Our concept, which has rather two-dimensional character, is to estimate transparency of the configuration to the "radiation" of the hard particles of different sizes, in the form of the anti-percolation function P. To construct this function we undertake the following steps. As first, spherical bullets of different sizes are "thrown" at a target, which is formed by the investigated configuration. If the bullet hits any of the particle from the system then it is regarded as reflected. Otherwise, the bullet goes through the target undisturbed. The anti-percolation function is constructed from the collected

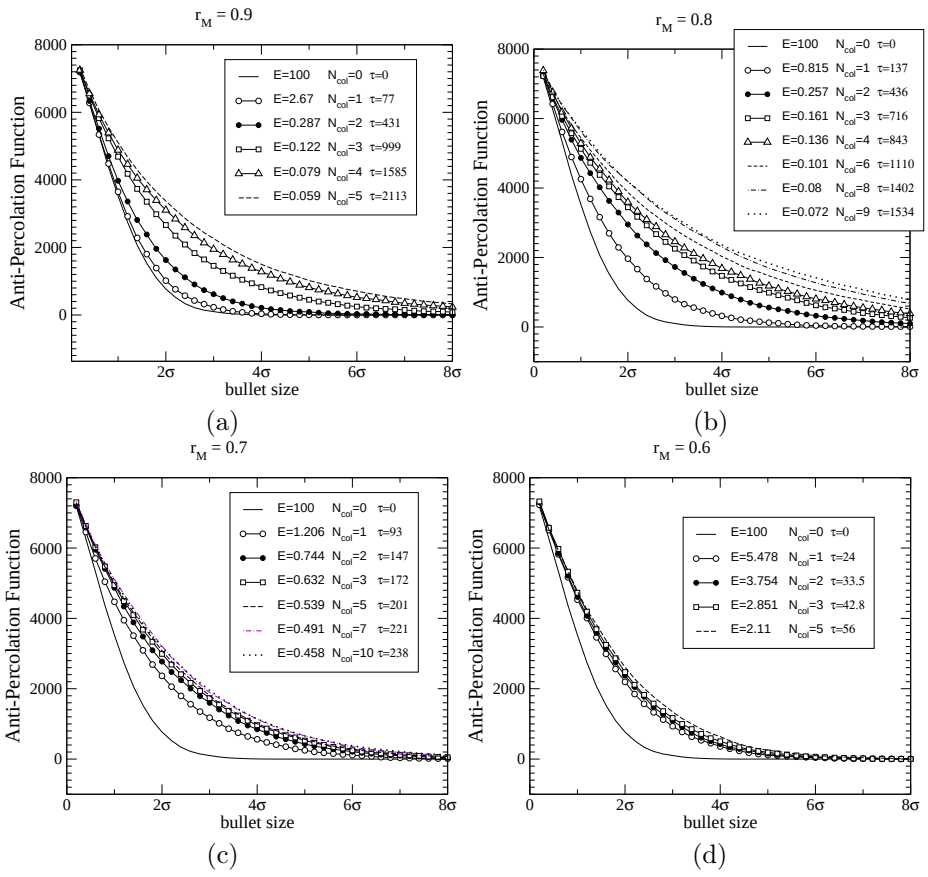

Fig. 7. The anti-percolation functions obtained for inhomogeneous configurations from the simulations performed under different dissipation conditions, given by the restitution parameter r_M. In the legends the following values are given: E — the total percentage measure for the energy per particle, N_{col} — the number of collisions after which the configuration has been considered for the analysis and the corresponding to these configurations dimensionless time τ (14).

number of the bullets, which have passed through the target. This function depends on the size of the bullet, $P(\sigma_{\mathrm{B}})$, and on the bullet number used, in our case it was 10000. The size of the bullets changes from $\sigma_{\mathrm{B}} = 0.2\sigma$ to $\sigma_{\mathrm{B}} = 8\sigma$, where σ is the diameter of the system disks. The expression "anti-percolation" has been here chosen, instead of simply "percolation", to account for the fact that when the bullet size increases then the function values decrease and finally drops to zero.

It turns out that for 10000 bullets the obtained anti-percolation functions are sufficiently smooth. In Fig. 7 we present these functions at different stages of cooling and for different restitution parameters. It is well seen that if the system contains large clusters, when it also contains large voids free of any particle, then the larger bullets have more chance to pass through the system, so the anti-percolation functions gain nonzero values for larger $\sigma'_{\mathrm{B}}s$. This process is well seen in the first two panels (a) and (b), which are obtained for r_M from the clustered regimes. (Comparing r_M to r from [5], by the use of Eq. (13), note that the kinetic regime occurs for $r_M \subset [0.99; 1.0]$, the shearing state for $r_M \subset [0.915; 0.985]$, the clustering state for $r_M \subset [0.795; 0.91]$. Also when $r_M < 0.795$ the system can be in the clustered state if not the simulation is halted by the inelastic collapse.)

A systematic change of P is apparent while the clusters gradually grow. In the panels (c) and (d) of Fig. 7 the restitution parameters used are taken from the regions, where the multiparticle collisions prevail and the cooling process is slower. There is no illustration of P for $r_M = 0.51$, since in this case the inelastic collapse does not allow to make progress in the simulations.

More details can be seen if P is presented on the logarithmic scale, as in Fig. 8. Here, in the panel (a) and (b) one can notice that in the state where the clusters are well formed, the anti-percolation function is a single exponent and its presentation on the logarithmic scale forms straight lines. This feature seems to be a general for the clustered state. One observes also that two systems with the same energy may be quite different as far as the cluster formation is concerned. An immediate conclusion occurs that the parameter of energy is not sufficient to describe the degree of clusterization. The dotted line from (b) and the line with triangles from (a), for which cases the energies are comparable, have completely different positions.

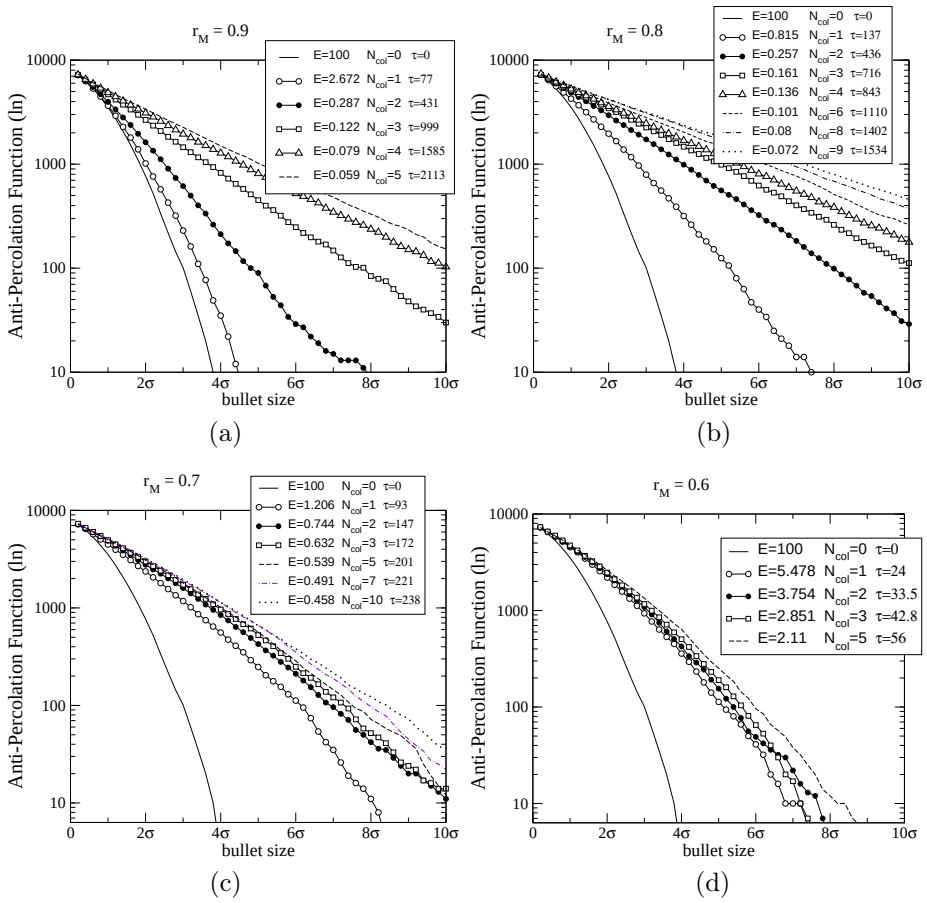

Fig. 8. The logarithm of the anti-percolation functions P obtained for inhomogeneous configurations from the simulations performed under different dissipation conditions, given by the restitution parameter r_M. In the legends the following values are given: E — the total percentage measure for the energy per particle, N_{col} — the number of collisions after which the configuration has been considered for the analysis and the corresponding to these configurations dimensionless time τ (its definition is given by (14)). For $r_M = 0.9$ ($r = 0.8$) and $r_M = 0.8$ ($r = 0.6$), which belong to the clustered regime, the logarithms of P form the straight lines indicating exponential character of the function.

6. Collision of two clusters

In this section we would like to present a collision of two clusters. Since one of our task were the animations of the clustered state, we had to resort to the simulations of smaller systems, in particular consisting of 10000 particles.

The animations prepared can be downloaded from [24]. Please note that even though they are not long and the system studied is rather small, the files with animations are large.

In this section, however, we can present some snapshots from the animated films. In Fig. 9 we show the collision of two clusters that has been encountered during the simulation with $r_M = 0.88$.

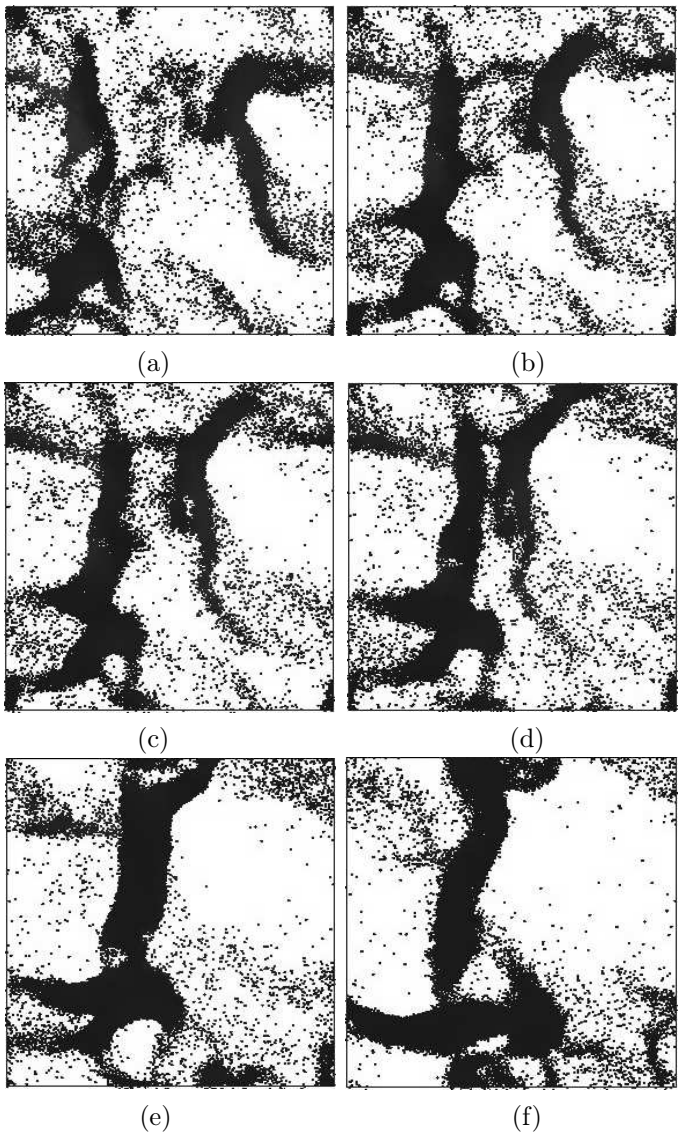

Fig. 9. The collision of two clusters.

In the panels (a) and (b) one observes two well formed clusters of elongated shapes, which approach each other. In the panel (c) the clusters are even closer and in (d) they are about to collide. In fact this is the cluster on the right hand side, which moves to the left. The cluster on the left almost does not change its position. In the panel (e) we have already one big cluster and in (f) the big cluster becomes thinner.

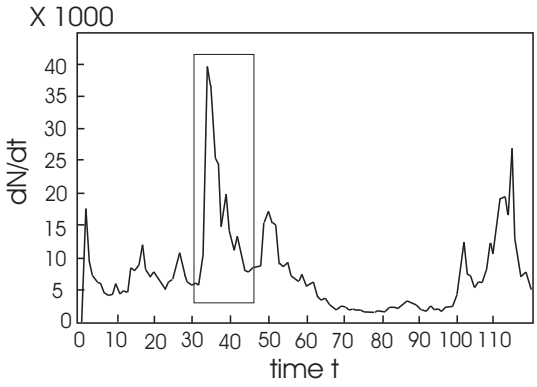

Fig. 10. The collision rate dN/dt for the part of the system evolution where the collision of two clusters (presented in Fig. 9) takes place. When two clusters collide then many particles meet each other in the short time and the collision rate abruptly grows (see details in the rectangular box).

It is also worth looking to realize how this phenomenon, the collision of two clusters, manifests itself in the physical variables that are usually monitored during simulations. For this purpose we present in Fig. 10 the collision frequency (the time averaged number of collisions) dN/dt. The area highlighted in the box in the middle of the picture corresponds to the collision presented in Fig. 9. A sequence of sharp peaks occurs here at the point, when two clusters are merging and refer to a multiparticle event, in which, however, the principle of the binary collision still holds.

7. Breakup of the band-clusters

In Fig. 11 we present the illustration of the kinetic process, which leads to the breaking of the granular band (stream of the particles). The first panel presents a well-formed, thick band. From the panels (b), (c) and (d) one sees that the particles move along the band, which becomes longer and thinner. Note also that at the same time the number of particles in the vicinity of the stream does not remarkably change, which suggest that the particles within the band do not escape from it and only move along the chain. Only when the

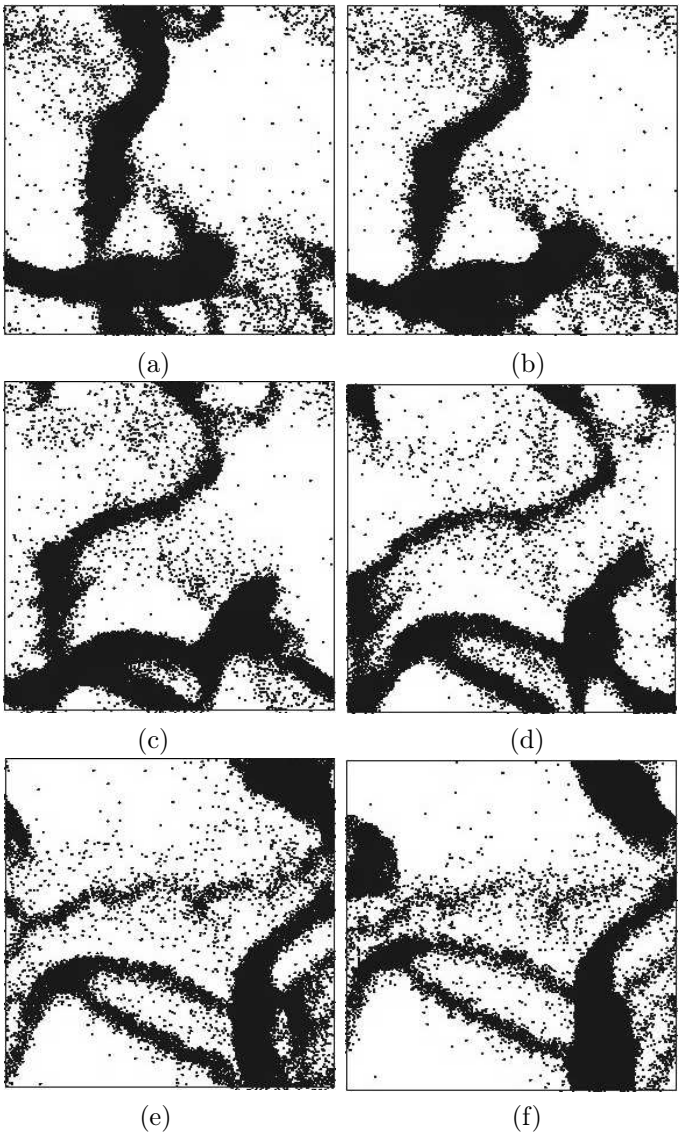

Fig. 11. Breakup of the granular band. The thick band form the panel (a) is being stretched with time. Intermediate stages are given in (b), (c) and (d). In the panel (e) the band is already hardly visible and in (f) one can notice only a sea of particles in the place where the band was observed before.

band is very thin, have the particles possibility to escape into the direction perpendicular to the band. This behavior, stretching of the chain, must have its own reason. Apparently, its is caused by the fact that the ends of the

chains are anchored to the clusters, which move into opposite directions. In the panel (a) the bottom end of the chain moves to the left and the upper end moves to the right. In the panel (e) these ends are no longer "bottom" and "upper", but find themselves to the left and to the right of the picture. In (f) one sees that the right anchor no longer exists. In Fig. 11 one can also find a structure, the thick bottom cluster, which upon cooling reorganizes into two bands encompassing a sort of empty pond. This process is originated by a density fluctuation, which has resulted in small empty space within the cluster (seen as the white spot at the bottom in the panel (b)). One realizes then that the observed tendency of band structure in the clustered state is just the result of the above two factors: density fluctuations within clusters and the stretching forces that occur at the anchoring points between two clusters moving in opposite directions. Figure 11 is the continuation of the cluster migration presented in Fig. 9 for $r_M = 0.88$.

After examination of many animations of the clustered state we got convinced that the above mentioned two factors are indeed the most important factors of the evolution.

8. Discussion and conclusions

In the present paper we have applied two new numerical methods to study the clusterization process in the two-dimensional hard disks system. The first method is based on the nearest neighborhood density, the concept of which has been already introduced in the case of the hard needles systems [17]. Here, it considers circular neighborhoods to each of the particle in the system. The density function is constructed by calculating the neighborhoods with the same number of disks. In the elastic case this function has the shape of the Gauss function. In the presence of clusters the neighborhood density function becomes asymmetrical with the part on the side of higher densities being the more pronounced the larger clusters are. Another property, which reflects the degree of the clusterization, is the anti-percolation function. This function is constructed from the number of circular bullets of different sizes, which are thrown at the system at random and which have not hit any particle from the system. One observes that for large restitution parameters the anti-percolation functions in the clustered state have exponential character. We have also presented illustrations of two characteristic events from the clusters dynamics: the collision of two clusters and the breakup of the granular band. The latter event takes place if two ends of the band are "anchored" to the parts of the system that are moving in opposite directions or have different collective velocities.

Animations showing different evolutions of granular streams can be found on the web page `http://pellegrina.strefa.pl/granulaty/granulki.html`

REFERENCES

[1] *Physics of Dry Granular Media — NATO ASI Series E 350*, eds. H.J. Herrmann, J.-P. Hovi, S. Luding, Kluwer Academic Publishers, Dordrecht 1998.

[2] *Granular Gases, Lectures Notes in Physics 564*, ed. T. Pöschel, S. Luding, Springer, Berlin 2001.

[3] *Continuous and Discontinuous Modelling of Cohesive Frictional Materials, Lecture Notes in Physics 568*, eds. P.A. Vermeer, S. Diebels, W. Ehlers, H.J. Herrmann, S. Luding, E. Ramm, Springer, 2001.

[4] *Powders and Grains*, ed. Y. Kishino, Rotterdam, Balkema 2001.

[5] S. McNamara, W.R. Young, *Phys. Rev.* **E53**, 5089 (1996).

[6] S. Luding, H.J. Herrmann, *Chaos* **9**, 673 (1999).

[7] I. Goldhirsch, G. Zanetti, *Phys. Rev. Lett.* **70**, 1610 (1993).

[8] I. Goldhirsch, M.L. Tan, G. Zanetti, *J. Sci. Comput.* **8**, 1 (1993).

[9] R. Cafiero, S. Luding, H.J. Herrmann, *Phys. Rev. Lett.* **84**, 6014 (2000).

[10] X. Nie, E. Ben-Naim, S. Chen, *Phys. Rev. Lett.* **89**, 204301 (2002).

[11] S. Miller, S. Luding, *Phys. Rev.* **E69**, 0313005 (2004).

[12] J.T. Jenkins, M.W. Richman, *J. Fluid Mech.* **192**, 313 (1988); *Phys. Fluids* **28**, 3485 (1985); *Arch. Ration. Mech. Anal.* **87**, 355 (1985).

[13] S. McNamara, *Phys. Fluids* **A5**, 3056 (1993).

[14] P. Deltour, J.L. Barrat, *J. Phys. I* **7**, 137 (1997).

[15] R. Brito, M.H. Ernst, *Europhys. Lett.* **43**, 497 (1998).

[16] J. Javier Brey, M.J. Ruiz-Montero, D. Cubero, *Phys. Rev.* **E60**, 3150 (1999).

[17] A. Chrzanowska, H. Ehrentraut, in *Dynamic Response of Granular and Porous Materials under Large and Catastrophic Deformations*, Springer, 2003, p. 315.

[18] B.D. Lubachevsky, *J. Comput. Phys.* **94**, 255 (1991).

[19] S. Miller, S. Luding, *J. Comput. Phys.* **193**, 306 (2004).

[20] D.C. Rapaport, *Comput. Phys. Rep.* **9**, 1 (1988).

[21] M.P. Allen, D.J. Tildesley, *Computer Simulations of Liquids*, Oxford University Press, New York 1987.

[22] P.K. Haff, in *Granular Matter*, ed. A. Mehta, Springer Verlag, Berlin 1994.

[23] S. Luding, E. Clement, A. Blumen, J. Rajchenbach, J. Duran, *Phys. Rev.* **E50**, 4113 (1994).

[24] `http://pellegrina.strefa.pl/granulaty/granulki.html`